Reactivity of High-Valent Iron–Oxo Species in Enzymes and Synthetic Reagents: A Tale of Many States

SASON SHAIK,* HAJIME HIRAO, AND DEVESH KUMAR†

Department of Organic Chemistry and The Lise Meitner-Minerva Center for Computational Quantum Chemistry, The Hebrew University of Jerusalem, Givat Ram Campus, 91904 Jerusalem, Israel

Received December 18, 2006

ABSTRACT

The Account discusses the phenomenon of two-state reactivity (TSR) or multistate reactivity (MSR) in high-valent metal–oxo reagents, projecting its wide-ranging applicability starting from the bare species, through the reagents made by Que, Nam, and collaborators, to the Mn(V)–oxo substituted polyoxometalate, all the way to Compound I species of heme enzymes. The Account shows how the behaviors of all these variegated species derive from a simple set of electronic structure principles. Experimental trends that demonstrate TSR and MSR are discussed. Diagnostic mechanistic probes are proposed for the TSR/MSR scenario, based on kinetic isotope effect, stereochemical studies, and magnetic- and electric-field effects.

Introduction

High-valent metal–oxo complexes are ubiquitous species used in nature and in the laboratory for the purpose of oxygenation of organic compounds. While iron is the most common metal in these species, there are also complexes with manganese–oxo, copper–oxo, and other moieties.[1] These species are formed in enzymes by O–O bond activation of O_2 or H_2O_2, depending on the class of enzymes, or synthetically by use of oxygen donors, e.g., PhI=O, which transfer oxygen to the transition metal (Scheme 1).[2]

These species, in heme and non-heme systems,[2] seem to share mechanistic features; they cause bond activation leading to unstable intermediates, e.g., by abstraction of hydrogen from alkanes, proton abstraction coupled with electron transfer (PCET) from phenols,[3] π-cleavage of C=C double bonds, etc. The initial bond activation is then followed by oxygen transfer from the transition metal–oxygen species to the organic intermediate, as in alkane hydroxylation by cytochrome P450,[4] or the radical itself will undergo oligomerization reactions as in plant peroxidases.[3]

The importance of metal–oxo species cannot be overstated, and the interest in their reaction mechanisms matches this distinction. Since an experimental proof of mechanism is not a simple matter, mechanistic bioinorganic chemistry has evolved with significant interplay of experiment and theory. In this sense, theoretical chemistry, specifically density functional theory (DFT) and hybrid DFT/molecular mechanics (DFT/MM) calculations,[4,5] has been playing an essential role in providing mechanistic data and structures of unstable intermediates and in deriving useful concepts.

An important role of theory is to provide insight and paint global pictures. In this sense, the two-state reactivity (TSR) and multistate reactivity (MSR) concepts[4,6] have emerged in response to intriguing experimental data, which have indicated that oxygenation reactions by enzymes like P450 and synthetic transition metal–oxo reagents behave as though more than one oxidant species were involved in the process. This apparent observation has generated lively mechanistic debates,[4,7] which are reminiscent of the heydays of physical organic chemistry, where intellectual chemistry figured prominently. In oxygenation reactions by P450, the recognition of TSR and MSR in 1998[8] eventually led to resolution of enigmatic issues and to predictions of novel mechanistic features.[4,7] Since, in the meantime, the TSR/MSR scenario has been repeatedly produced by theory in a variety of processes, including enzymes[3] and synthetic reagents,[9] our purpose here is to highlight the wide-ranging applicability of the concept and its insight into reactivity, to draw generalities, and to suggest mechanistic probes of TSR/MSR scenarios.

TSR/MSR Scenarios in Bond Activation Reactions

Figures 1–5 show TSR/MSR scenarios in five different systems. All these cases share one common feature; they involve energy profiles of at least two spin states that either criss-cross or remain in proximity. This is the fundamental feature of the TSR/MSR scenario, whereby different states coproduce different reaction intermediates and products in a given process. The figures also exhibit differences, which we would like to understand and generalize.

Figure 1 depicts the energy profiles for the gas-phase conversion of H_2 to water by FeO^+.[10] The figure exhibits doubling of the energy profile into sextet [high-spin (HS)] and quartet processes [low-spin (LS)], where the LS state crosses below the HS transition state and hence potentially mediates the transformation. This figure is an archetype

Sason Shaik is a quantum chemist, a former student of Nicolaos Epiotis, and a former postdoc of Roald Hoffmann. His current interests are in developing general concepts for bonding and reactivity and in modeling of metalloenzymes and bioinorganic reactions.

Hajime Hirao is a native of Japan and a student of Tomohiko Ohwada. He is at present a JSPS postdoc of S. Shaik. His interests are in method development and in structure and reactivity in bioinorganic chemistry.

Devesh Kumar is a native of India and a student of Mihir Roychoudhury. He was a postdoc of S. Shaik and is currently a postdoc of W. Thiel. His present interests are in modeling cytochrome P450.

* To whom correspondence should be addressed. Telephone: +972 (0)2 658 5909. Fax: +972 (0)2 658 4033. E-mail: sason@yfaat.ch.huji.ac.il.

† Current address: Max-Planck-Institut für Kohlenforschung, Kaiser-Wilhelm-Platz 1, D-45470 Mülheim an der Ruhr, Germany.

10.1021/ar600042c CCC: $37.00
Published on Web 05/09/2007

Scheme 1. O–O Bond Activation in Iron-Based Complexes and Enzymes

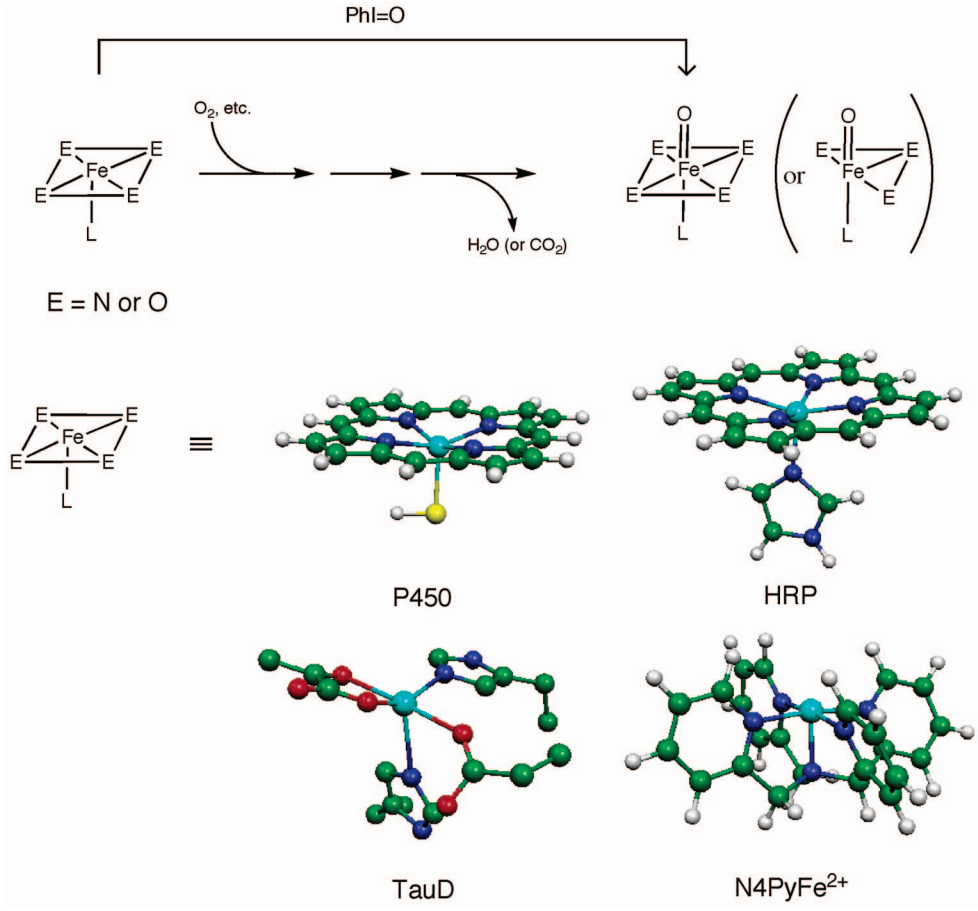

of the energy profiles corresponding to the activation of alkanes by transition metal–oxo cations.[6a,c,11,12]

Figure 2 shows a C–H hydroxylation reaction by the active species of the enzyme cytochrome P450, so-called Compound I (Cpd I). Panel (a) shows the gas-phase mechanism,[13,14] while panel (b) shows the mechanism by which the bulk polarity of the protein is mimicked using a low dielectric constant ($\varepsilon = 5.7$) and the amidic NH–S interactions with the thiolate ligand of Cpd I in P450s[15] are modeled by addition of two NH_3 molecules.[4,14] Figure 2a exhibits doublet- and quartet-state profiles that are roughly parallel throughout the H-abstraction step. Subsequently, the doublet intermediate "rebounds" and forms an alcohol complex in a barrier-free manner, while the quartet intermediate faces a barrier to rebound. There is also a low-lying sextet-state surface that behaves like the quartet surface. Notably, the H-abstraction transition states ($\mathbf{TS}_{\mathrm{H}}$) carry Roman numerals that indicate the different oxidation states of the iron center. Figure 2b shows that the interactions of Cpd I with the "environment" bring more states into the act,[14] some with Fe(III) others with Fe(IV). The doublet states exhibit effectively concerted processes with barrier-free rebounds, while the quartet states have stepwise mechanisms with barriers to rebound. This reactivity scenario was termed MSR to signify the multitude of states that contribute to product formation.

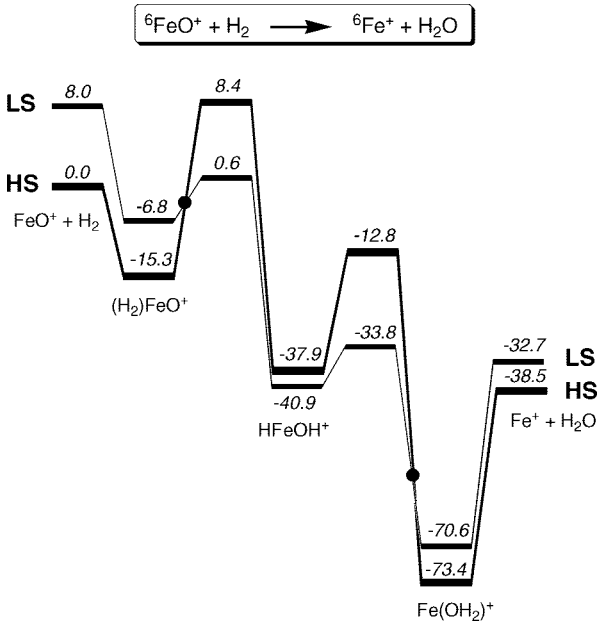

FIGURE 1. DFT(B3LYP)-calculated TSR scenario in the gas-phase oxygenation of H_2 by FeO^+.[10] The labels HS and LS indicate the relative spin quantum number.

Figure 3 shows the MSR scenario in styrene epoxidation by Cpd I.[16] Here too, a few states run parallel through the C=C activation phase and then produce HS quartet and LS doublet organic radical and cationic complexes. Thus,

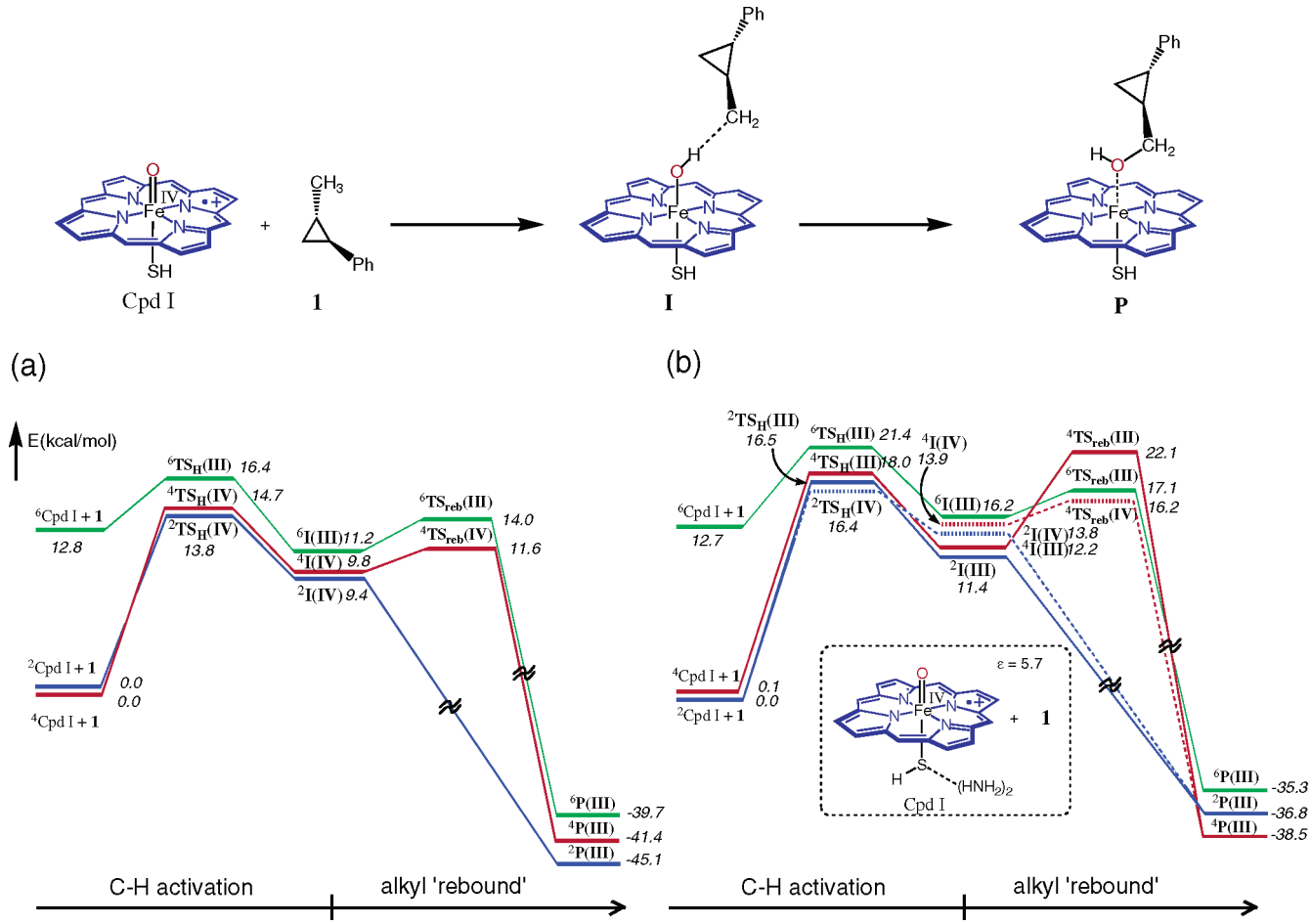

FIGURE 2. DFT(B3LYP/LACVP)-calculated TSR/MSR scenarios in the C–H hydroxylation of **1** by Compound I of P450: (a) in the gas phase and (b) with NH–S interactions (included in geometry optimization) and bulk polarity effect. Relative energies include ZPEs.

Figures 2 and 3 share a common behavior: the HS mechanisms are stepwise with sufficiently long lived intermediates, while the LS mechanisms are effectively concerted with ultrashort lived intermediates. All heme systems investigated by us possess similar features irrespective of the axial ligand (thiolate as in P450 or imidazole as in HRP or microperoxidases).

Figure 4 shows a manganese–oxo complex, made from the polyoxometalate cage $[PW_{12}O_{40}]^{3-}$ via replacement of one W=O moiety with a Mn^{V}=O moiety. Such a reagent was recently characterized by NMR and shown to possess a singlet ground state, and to perform C–H and C=C activations.[17] The figure exhibits an MSR scenario in the allylic hydroxylation of propene, which is mediated by the triplet and quintet states that cut through the high singlet-state barrier.

By now we have calculated the reactivity of some 10 different L_5Fe^{IV}=O reagents made[18] with the polydentate nitrogenous ligands. Figure 5 shows a typical TSR/MSR scenario, with C–H activation and rebound, in the hydroxylation of cyclohexane (**CH**) by $[N4Py]Fe^{IV}O^{2+}$.[9] It is seen that the quintet state cuts below the barrier of the ground triplet state and mediates the transformation. Note that, unlike before, here the HS process is effectively concerted.

Taken together, Figures 1–5 exhibit an impressive collage of processes that share the common feature of spin-state crossing and entanglement. Can we make sense of these features and generalize the picture? Do these features have characteristic mechanistic impact? In the following sections, we address these questions.

Origins of TSR/MSR Scenarios

Transition metals have five d orbitals that are close in energy, with energy spacing depending on the strengths of the ligand–metal interactions. Sometimes the ligands have high-lying orbitals close to the d block orbitals.[4] Additionally, during bond activation, the organic substrate develops high-lying orbitals close to the d block. As such, the number of closely lying orbitals that are not doubly occupied is large and becoming larger as the reaction progresses, hence giving rise to a dense manifold of states. The other factor is the exchange interaction between the electrons in d orbitals, e.g., 20 kcal/mol on Fe, which favors high-spin situations.[9,19] Taken together, metal–oxo reagents involve a dense manifold of states differing in orbital occupancy, transition metal and ligand oxidation states, and spin quantum numbers. In general, these states will remain close along the reaction pathways, and as their

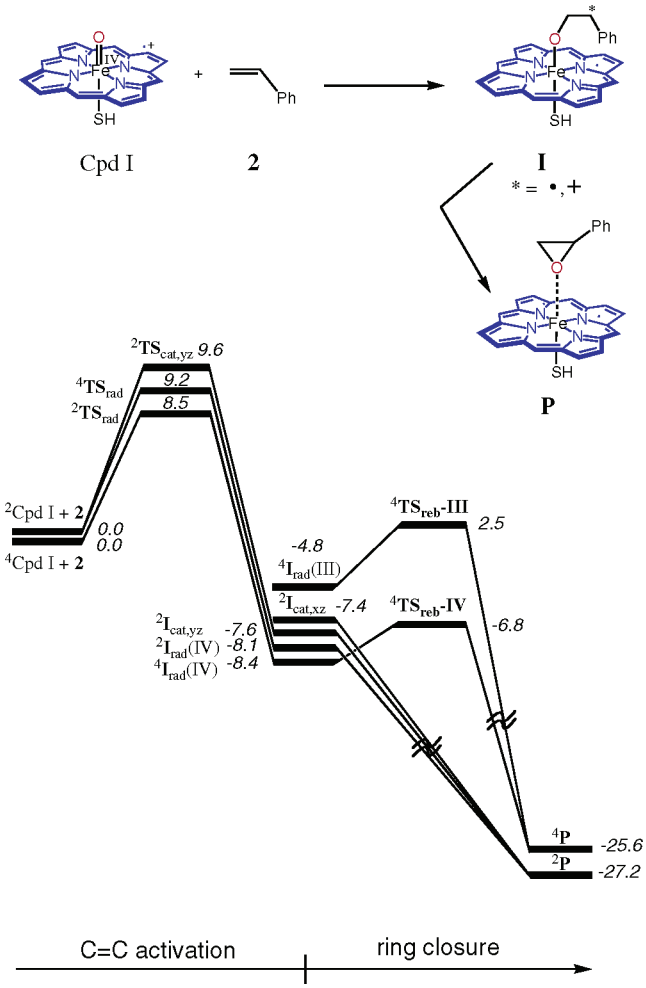

FIGURE 3. B3LYP/LACVP(+ZPE)-calculated MSR scenario during styrene epoxidation by Compound I.[16]

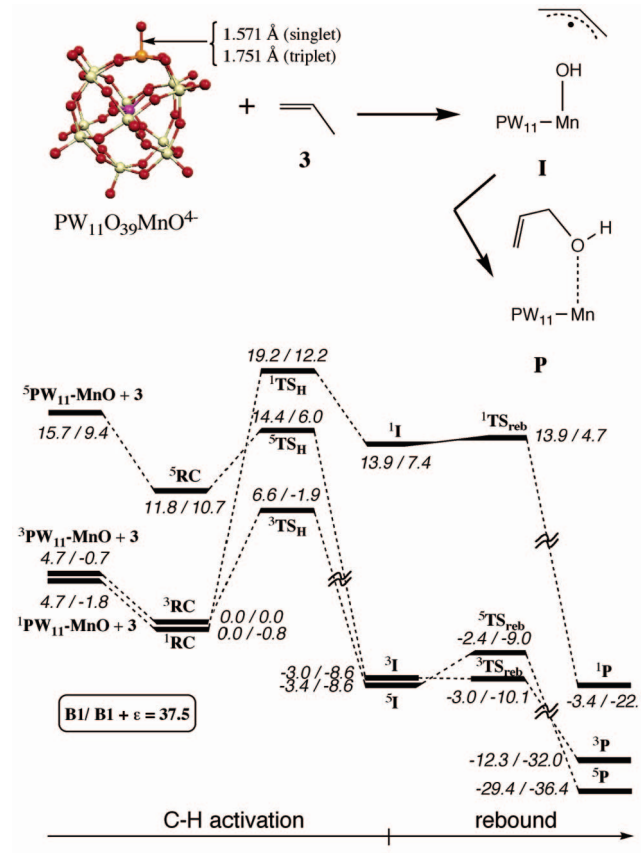

FIGURE 4. BLYP-calculated MSR scenario during allylic hydroxylation of propene by $[PW_{11}O_{39}\text{-}Mn^{V}{=}O]^{4-}$ ($PW_{11}MnO$). Energies are reported for a gas phase and an acetonitrile solution ($\varepsilon = 37.5$).[17] RC is the reactant complex.

number increases, when orbitals of the molecule undergoing oxidation become accessible, one obtains the TSR/MSR scenarios as in Figures 1–5. The following analyses illustrate these factors.

Figure 6a shows orbitals and low-lying states of $[N4Py]Fe^{IV}{=}O^{2+}$.[9] This d block spreads into the three-below-two pattern typical of distorted octahedra; the group of three has a low-lying δ orbital and two π^* orbitals with antibonding $Fe(d_\pi)-O(p_\pi)$ character, while the group of two involves σ^* antibonding orbitals, one with the equatorial nitrogen lone pairs and one with the two axial ligands. With oxidation state IV, the d block contains four electrons; the ground state has the $\delta^2\pi^{*1}\pi^{*1}$ configuration with a triplet spin quantum number ($S = 1$), and the corresponding singlet state ($S = 0$) lies higher by 8.4 kcal/mol. These states are analogues of the triplet and singlet states of O_2, and this is common to all iron–oxo complexes, which maintain the stable triplet $\pi^{*1}\pi^{*1}$ FeO configuration.[1,3,4,6,8,9,12,19] A low-lying state is the quintet ($S = 2$)[18] $\delta^1\pi^{*1}\pi^{*1}\sigma^*_{xy}{}^1$ configuration; its energy relative to $S = 1$ is a balance between the large $\delta \rightarrow \sigma^*_{xy}$ orbital energy gap, determined by the N–Fe interaction strength, favoring $S = 1$, and the five new d–d exchange interactions[19] (20 kcal/mol each) that favor $S = 2$.[9] On balance, this creates a small energy gap between the two states and sets the stage for TSR.

The transformation of these two states along the reaction pathway is represented by the orbital diagram[9] in Figure 6b. It depicts the changes in orbital occupancy using the oxidation-state formalism; in this formalism, the substrate undergoing oxidation donates two electrons to the iron–oxo complex. These diagrams are represented in three panels, corresponding, from left to right, to the reactants, the intermediate ($^{2S+1}$**I**), and the product ($^{2S+1}$**P**). Thus, with the triplet state as the beginning, as H-abstraction occurs, one electron shifts from the σ_{CH} orbital of the alkane to a π^*(FeO) orbital, and a spin develops on the alkyl radical due to the singly occupied orbital, ϕ_C, in intermediate ^{3}**I**. Subsequently, as the alkyl radical rebounds, the electron shifts from ϕ_C to the $\sigma^*_{z^2}$ orbital and generates the alcohol complex, ^{3}**P**. On the quintet surface, the H-abstraction is attended by an electron shift from σ_{CH} to $\sigma^*_{z^2}$. Now an electron with spin up is shifted to increase the rate of exchange on the iron by four new d–d interactions.[9] This large exchange stabilization lowers the quintet barrier below the triplet state and leads to their crossing (Figure 5). In the rebound step, starting from ^{5}**I**, the electron shifts from ϕ_C to the δ orbital of the iron–hydroxo complex. Since the δ orbital is low-lying, there will be no barrier to rebound on the quintet surface. By contrast, on the triplet surface, the

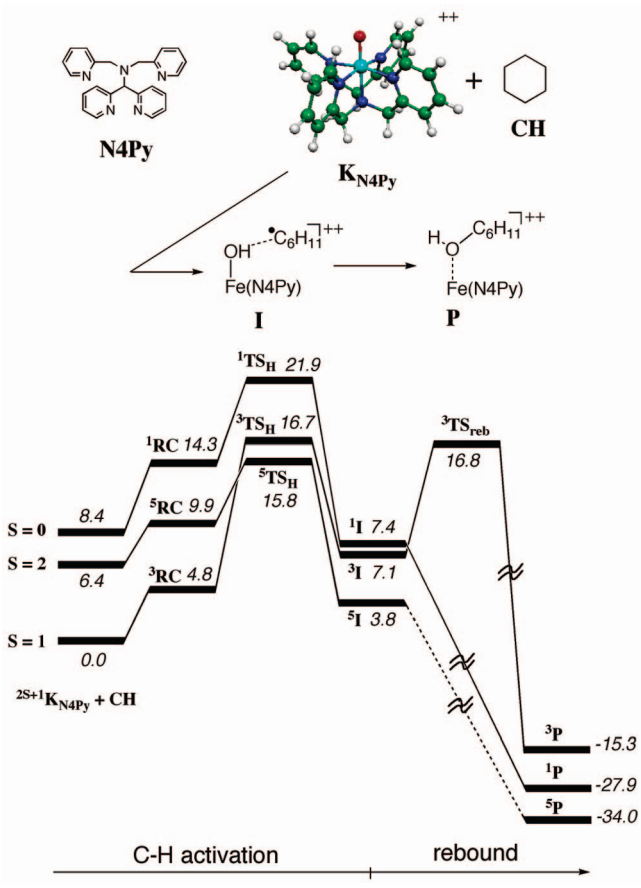

FIGURE 5. B3LYP/LACV3P++**//LACVP-calculated TSR/MSR scenario during hydroxylation of cyclohexane by $[N4Py]Fe^{IV}O^{2+}$.[9] Relative energies include ZPEs and solvation energies in acetonitrile (ε = 37.5).

electron shifts, during rebound, to the high-lying $\sigma^*_{z^2}$ orbital (without much gain of exchange), and therefore, the triplet state features a significant barrier. As such, we obtain in Figure 5 a TSR scenario, with a triplet-state mechanism that has a large H-abstraction barrier and a significant rebound barrier, and an effectively concerted quintet mechanism that cuts through the triplet barrier.

The orbital diagram in Figure 6a can be used to explain also the MSR scenario of the Mn(V)=O complex in Figure 4. Now, the ground state is a singlet with two electrons on the lowest-lying δ orbital. With no electrons in the π^*(MnO) orbitals, the Mn=O bond of this state is short and strong (Figure 4).[17] Therefore, the singlet state will have a high barrier to bond activation. The process will be mediated by higher-spin states, which possess long and hence activated Mn=O bonds.

Figure 7 shows the orbitals and low-lying states of Cpd I of P450.[4,14,20] Here, two porphyrin orbitals, a_{2u} and a_{1u}, are sufficiently high in energy (recall, the porphyrin periphery is "antiaromatic") to intermingle with the d block orbitals. Since the total oxidation state of the complex is V, the iron will be Fe^{IV}, while the porphyrin will assume the remaining oxidation equivalent as a cation radical. With a d^4 configuration, and one unpaired electron on porphyrin, the ground state, nascent from the $\delta^2\pi^{*1}\pi^{*1}a_{2u}{}^1$ configuration, has two spin states: quartet ($S = {}^3/_2$) and doublet ($S = {}^1/_2$), labeled as $^{4,2}A_{2u}$. However, the dense orbital block generates a manifold of states squeezed within 26 kcal/mol, e.g., $^2A_{2u}$ where the two electrons in the $\pi^{*1}\pi^{*1}$ configuration are paired into a singlet state, $^{2,4}A_{1u}$ states,[21] and Fe^V=O states, where one electron from the $\delta^2\pi^{*1}\pi^{*1}$ configuration goes to fill the a_{2u} orbital of the porphyrin. In addition, the exchange d–d interaction plays its role and generates $^{6,4}A_{2u}$ states with a $\delta^1\pi^{*1}\pi^{*1}a_{2u}{}^1\sigma^*_{xy}{}^1$ configuration, and within 14 kcal/mol of the ground states. What a rich manifold of states!

The orbital evolution diagram in Figure 8 focuses on the species nascent from the doubly degenerate ground state, $^{2,4}A_{2u}$, during C–H hydroxylation (C=C epoxidation).[4,7] In the course of H-abstraction (C=C activation), an electron shifts from the σ_{CH} (π_{CC}) orbital to one of the singly occupied orbitals of Cpd I and generates four intermediates. Shifting the electron to a_{2u} creates the $^{2,4}\mathbf{I}_{rad}$(IV) intermediates having Fe^{IV} centers, while shifting it to π^*(FeO) generates the $^{2,4}\mathbf{I}_{rad}$(III) intermediates with Fe^{III} centers and porphyrin radical cations.

In the rebound (ring closure) steps, the electron will shift from ϕ_C to the heme to form the ferric–alcohol (epoxide) complexes [^{2,4}**P**(III)]. In the $^2\mathbf{I}_{rad}$(III) intermediate, the electron will shift to a_{2u}, while in $^2\mathbf{I}_{rad}$(IV), the electron will shift to $\pi_{xz}{}^*$(FeO), both cases leading to ^{2}**P**(III). By contrast, in the ^{4}**I** intermediates, spin conservation requires shifting electron(s) to higher-lying orbitals. In $^4\mathbf{I}_{rad}$(IV), the electron will shift to the $\sigma^*_{z^2}$ orbital, whereas in $^4\mathbf{I}_{rad}$(III), two electrons must shift to avoid spin frustration: one electron from ϕ_C to $\sigma^*_{z^2}$ while another, with spin down, from the filled π^*(FeO) to a_{2u}.[6b,7]

Since in the doublet manifold the electron is shifted to low-lying orbitals, these rebound (ring closure) processes are barrier-free, whereas the quartet-state processes which involve shifting electrons to the higher-lying $\sigma^*_{z^2}$ orbital face significant rebound barriers.[7] Furthermore, since the electronic reorganization involving $^4\mathbf{I}_{rad}$(III) rebound is more complex than that of $^4\mathbf{I}_{rad}$(IV), the rebound (ring closure) barriers nascent from $^4\mathbf{I}_{rad}$(III) will be higher than those from $^4\mathbf{I}_{rad}$(IV).[7] Reviewing Figures 2 and 3 shows that these are the computed patterns. Thus, the LS states proceed via effectively concerted mechanisms, while the HS states have stepwise mechanisms, with radical intermediates whose lifetimes depend on the oxidation state of iron in the complex; the radical in the $^4\mathbf{I}_{rad}$(III) intermediate is longer-living than the one in the $^4\mathbf{I}_{rad}$(IV) intermediate.

Note that shifting the second electron without creating the O–C bond would leave behind alkyl cations. Here again, the resultant doublet $^2\mathbf{I}_{cat}$(III) species collapses to the alcohol (epoxide) without a barrier (e.g., Figure 3). The quartet-spin intermediate will be higher in energy and longer-living and may lead to free carbocations[7,13] and other products as well.[16] As such, the reactivity scheme is rich with radicals and cations, in two spin manifolds and with different mechanistic behaviors.

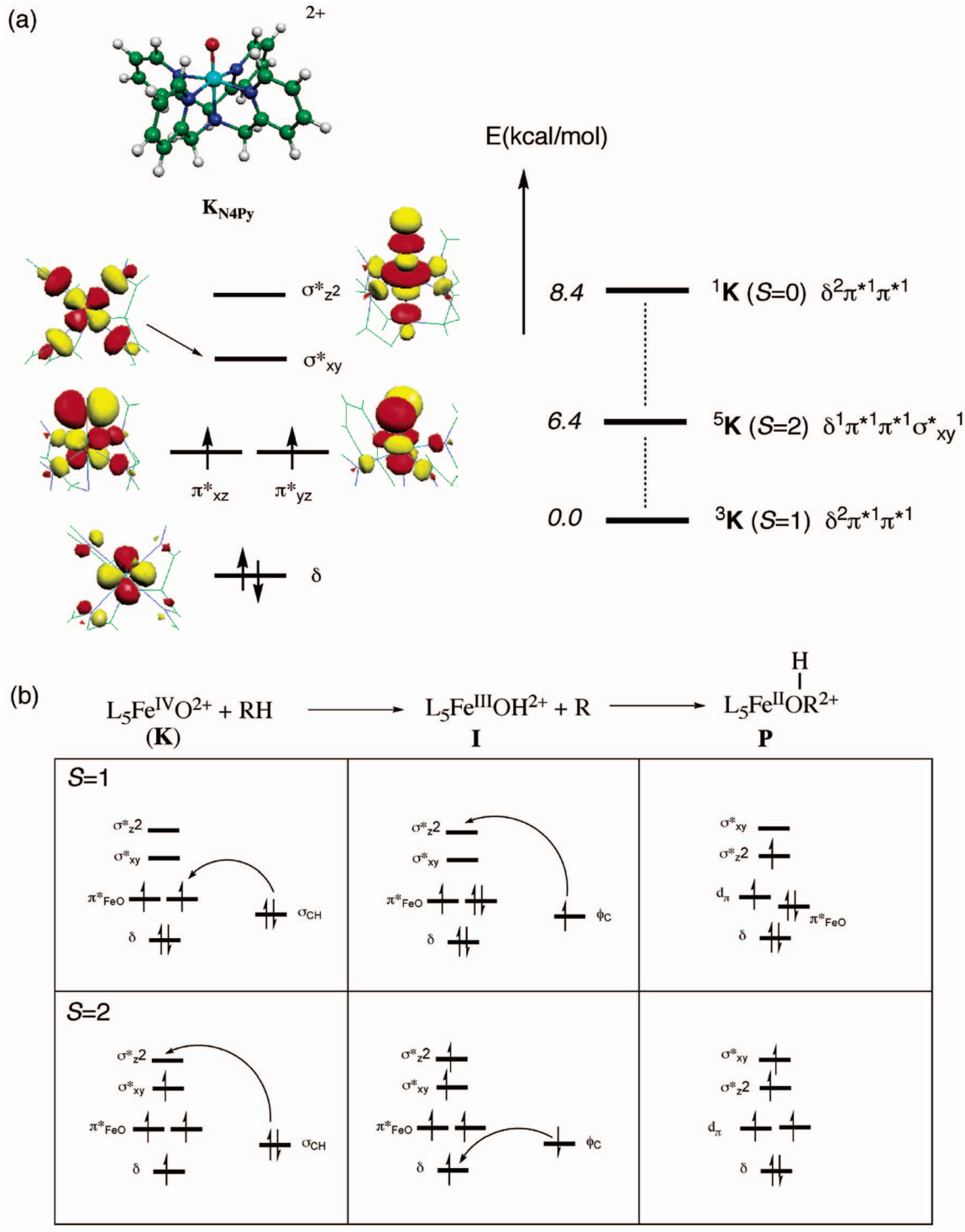

FIGURE 6. (a) Energy diagram of d block orbitals of [N4Py]Fe^{IV}=O^{2+} (**K**) and the low-lying spin states (S = 1, 2, or 0), with their B3LYP/LACV3P++**//LACVP relative energies in solution (ε = 37.5). (b) Orbital occupancy evolution during C–H hydroxylation.

Features of TSR/MSR Scenarios

While the effect of spin-state crossing on rates is occasionally important,[22,23] there are key aspects of TSR/MSR which arise from the fact that the participating states have different transition-state structures, different stereochemical or regiochemical preferences, and intermediates with different lifetimes. As discussed below, these scenarios will pose a challenge in mechanistic studies based on single-state reactivity concepts.

Catalysis by Spin Crossover. An example of this effect is the reaction in Figure 1.[6a,c;10–12] Thus, since the HS TS lies well above the threshold energy of the reactants, the HS reaction is in fact gas-phase "forbidden" at ambient temperatures. What enables oxidation of H_2 to water, at all, is the LS surface that cuts through the HS surface and mediates the bond activation process.[6a,c;10] What limits the efficiency of the reaction is the poor spin-orbit coupling interaction at the spin-inversion junctions in

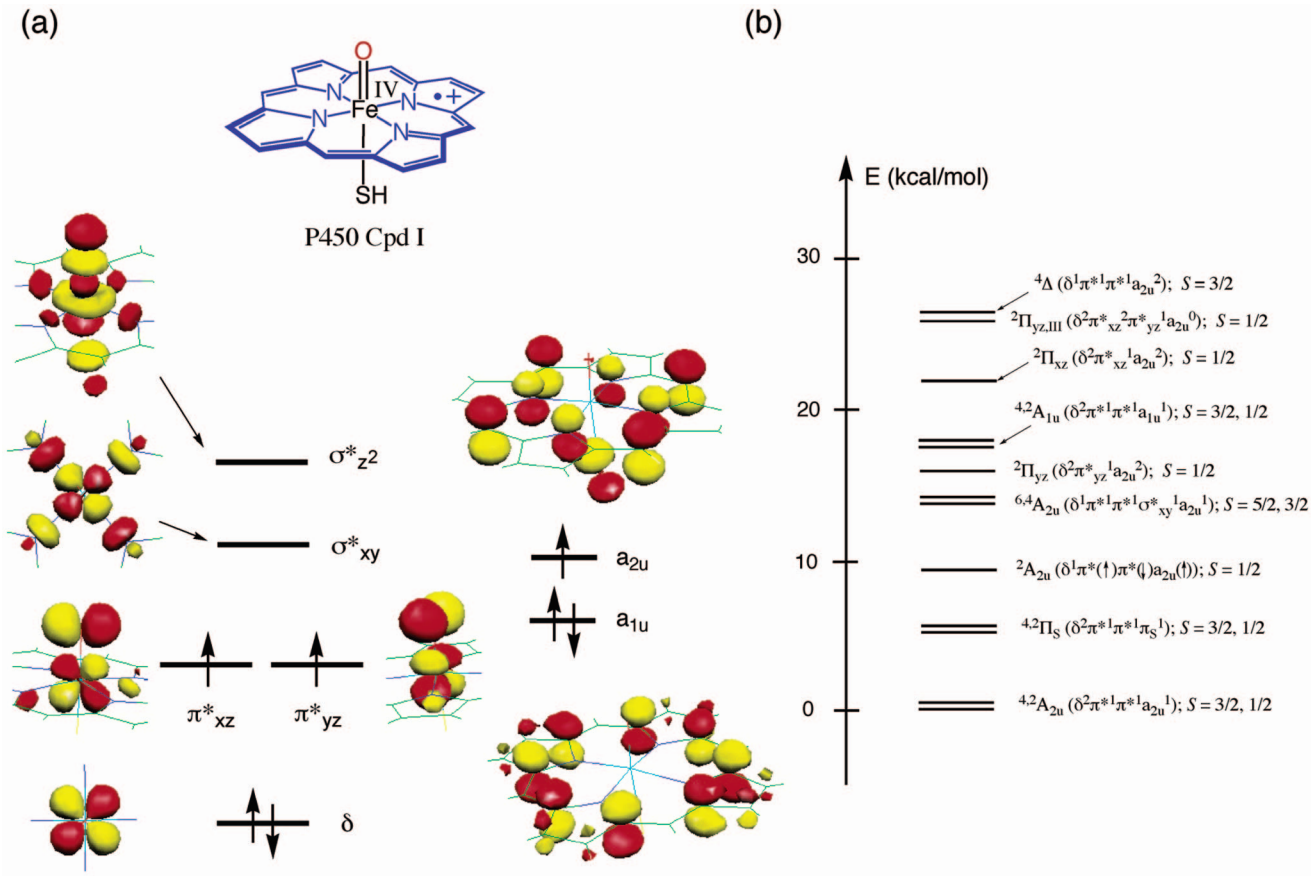

FIGURE 7. (a) Energy diagram of key orbitals of Cpd I of P450. (b) Low-lying states and their relative B3LYP energies in the gas phase.

Figure 1.[10,23] Nevertheless, without the LS–HS crossing, no oxidation would have occurred at ambient temperatures! Note that the hydroxylation reactions mediated by [N4Py]–Fe^{IV}=O^{2+} (Figure 5),[9] $PW_{11}O_{39}$–Mn^{V}=O^{4-} (Figure 4),[17] etc.,[9] also exhibit "catalysis" by spin crossover.

Different Products from Different States. Another intriguing TSR feature is the fact that the two spin states prefer different mechanisms that produce different intermediates and products. This spin-dependent mechanistic phenomenon has been observed throughout the gamut of oxidation processes; from the simple reaction of FeO^{+} [10,24] to the complex mechanisms of enzymes and synthetic catalysts.[3,4,9,13,17]

In P450 oxygenation (Figures 2 and 3), the LS states lead to products via effectively concerted pathways while the HS states proceed by stepwise mechanisms with sufficiently long lived intermediates. As argued,[4,7] this dichotomy is behind the controversial lifetimes of the radical intermediates quantified by assuming product formation via a single reactive state. Thus, as illustrated in Figure 9a, in a single-state scenario the alkyl radical formed by H-abstraction can either rebound to give an unrearranged alcohol (***U***) or first rearrange and then rebound to form a rearranged alcohol (***R***). The apparent lifetime (τ_{app}) of the radical is then determined from the branching ratio [***R***/***U***] of the radical and the speed (k_R) of its rearrangement. However, the use of ultrafast radical probes (Figure 9b) for quantifying τ_{app}[25] produced unrealistically short lifetimes that could not support the presence of intermediates. Nevertheless, radical intermediates abound in this reaction,[2b,26] so what could be the source of this contradiction?

Figure 2 reveals that TSR is the source of these unrealistic apparent lifetimes. Thus, since the LS doublet state is effectively concerted, it will produce only unrearranged (***U***) products. By contrast, the stepwise HS processes will mainly produce the rearranged product (***R***). Therefore, the quantity [***R***/***U***] is a measure of the relative yields of the HS and LS processes and not a true measure of the branching of a single radical species into two products as required by the equation in Figure 9a. As such, for very fast radical clocks (as in Figure 9b), the [***R***/***U***] ratio will be determined primarily by the relative H-abstraction barriers on the HS-quartet and LS-doublet surfaces. Since ^{2}**TS$_{H}$** is lower than ^{4}**TS$_{H}$**,[4,7] the yield of the LS reaction is higher than the HS yield, and hence, [***R***/***U***] will predict a τ_{app} shorter than the real lifetime of the radical on the HS surfaces. Furthermore, modeling the rebound barrier predicts that[4,7] the HS barrier will gradually diminish as the radical center becomes a better electron donor; at some limiting donor capability, the barrier will vanish, thus making both HS and LS processes effectively concerted. Figure 10[4,7] depicts the TSR for the substrate where the methyl group is replaced with an isopropyl group, making the resulting radical a powerful donor. Now, the two states generate ferric–alcohol products in effectively concerted manners and are therefore predicted to produce

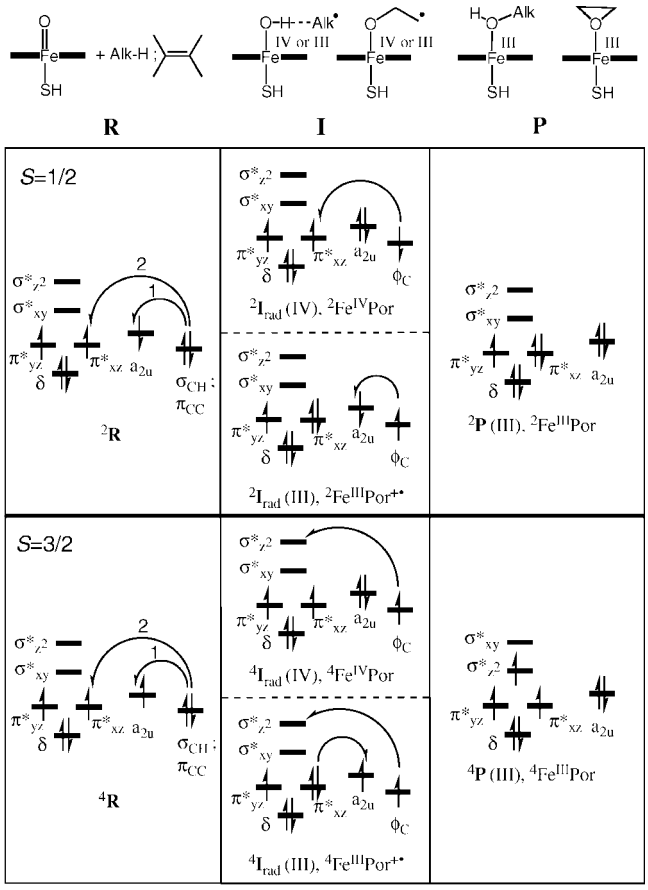

FIGURE 8. Orbital occupancy evolution during C–H hydroxylation (C=C epoxidation) by P450 Cpd I.

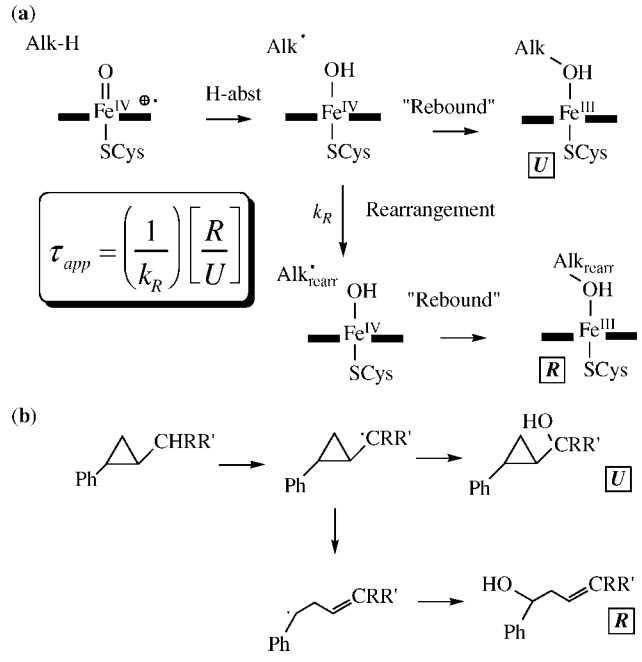

FIGURE 9. (a) Rebound mechanism and the apparent radical lifetime. (b) ***U*** and ***R*** products of ultrafast radical clocks.

no rearranged alcohols. Experimentally, the [***R***/***U***] quantity for this probe is <0.01.[25]

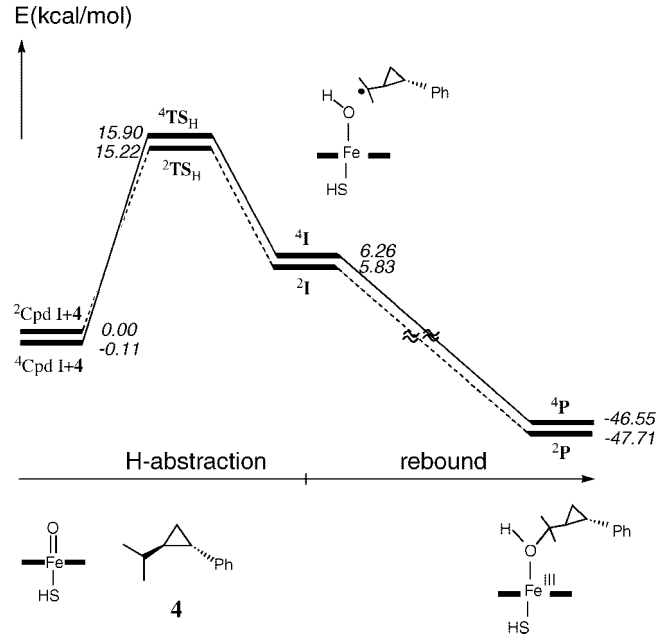

FIGURE 10. B3LYP/LACVP results for C–H hydroxylation of **4**.[13]

Scheme 2. TSR and SSR in Two Ends of a Single Molecule

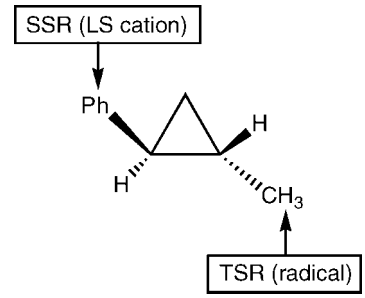

Let us highlight two more consequences of TSR/MSR scenarios. Thus, during C=C epoxidation (Figure 3), there are radical intermediates in the HS manifold with two different oxidation states on iron, namely, ^{4}**I**$_{rad}$(IV) and ^{4}**I**$_{rad}$(III). As reasoned above, the ring-closure barrier for ^{4}**I**$_{rad}$(III) is much larger. With a small barrier, the ^{4}**I**$_{rad}$(IV) state will lead mostly to epoxide products with scrambled stereochemistry [due to almost free C–C bond rotation in ^{4}**I**$_{rad}$(IV)], whereas the ^{4}**I**$_{rad}$(III) state will have sufficient lifetime to produce heme-alkylated and aldehyde complexes that require surmounting significant barriers.[4,16]

Sometimes, the energy difference between the LS and HS activation barriers is significant, leading therefore to a spin-selective single-state reactivity (SSR). An amusing case is the probe substrate *trans*-2-phenylmethanecyclopropane in Scheme 2. This substrate leads to hydroxylation of both the methyl and phenyl groups.[13] As we showed in Figure 2, the methyl group hydroxylation proceeds by TSR and MSR with radical intermediates. By contrast, the phenyl oxidation proceeds via a LS cationic Meisenheimer complex.[27]

Prospective: Probes of TSR and MSR

Experimental probing of TSR/MSR scenarios is challenging and would require the interplay of experiment and theory.

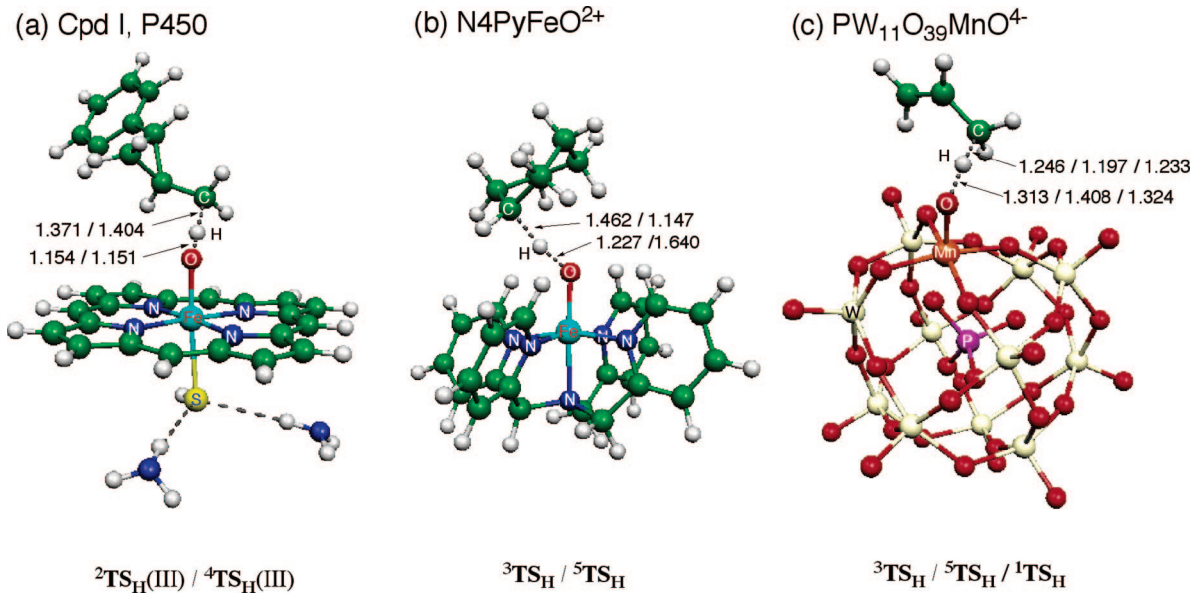

FIGURE 11. O–H–C distances (B3LYP/LACVP) for the $^{2S+1}$**TS**$_H$ species of (a) Figure 2b, (b) Figure 5, and (c) Figure 4.

Devising mechanistic probes for TSR/MSR or spin-selective chemistry requires both traditional and unconventional methods:

Measurements of [*R*/*U*]. Consider the C–H bond hydroxylation by the synthetic iron–oxo reagent in Figure 5. Here and in all other related reagents,[9] only the triplet-state surface exhibits a barrier to rebound while the quintet state features an effectively concerted process. This means that a fast radical probe (large rearrangement rate constant) on the triplet manifold will give rise only to ***R*** products, while the quintet-state reaction will lead exclusively to ***U***, thus enabling one to quantify the $[S = 1]/[S = 2]$ reactivity ratio.

Kinetic Isotope Effect Probes. In 1998, we showed that HS and LS processes for C–H bond activation exhibit different semiclassical kinetic isotope effect (KIE) values due to different TS geometries.[10] Figure 11 displays the spin-dependent O–H–C distances in $^{2S+1}$**TS**$_H$ species for C–H bond activation by three different metal–oxo species.[9,14,17] In fact, all the cases we studied possess spin-dependent O–H–C distances.[28] Since the KIE is sensitive to the location of the transition state along the H-transfer coordinate,[28] we expect different KIEs for different spin sates. This feature of the $^{2S+1}$**TS**$_H$ species can serve as a probe of spin-state reactivity.

Scheme 3 shows two examples of spin-dependent KIEs. In the gas-phase C–H bond activation of norbornane by FeO^+ (Scheme 3a), the activation of the C–H$_{endo}$ bond was found to involve a KIE value much smaller than that of the C–H$_{exo}$ bond.[29] This difference was demonstrated[29] to result from two different spin states: the LS quartet activating the *endo* C–H bond and the HS doublet the *exo* C–H bond. In the case of C–H bond hydroxylation of *N*,*N*-dimethylaniline by P450 Cpd I (Scheme 3b),[28] the computed KIE$_{LS}$ value is smaller than the corresponding KIE$_{HS}$. Only the KIE$_{LS}$ value fits the experimental KIE.[30] Theory shows[28] also that ^{2}**TS**$_H$ is 3.7 kcal/mol lower than ^{4}**TS**$_H$, and hence, the reaction will proceed exclusively via the

Scheme 3. KIEs in Two Examples of HS and LS C–H Bond Activations

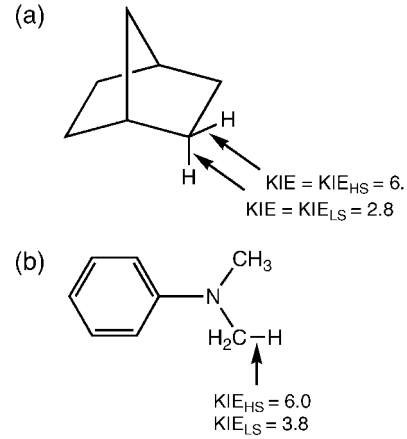

LS state. Similar, yet unpublished, results were obtained for C–H bond hydroxylation of trimethylamine and the series of para-substituted *N*,*N*-dimethylanilines discussed in ref 30. All these examples show that KIE measurement can be a probe of spin-selective chemistry.

A system that should exhibit spectacular KIE features is the C–H bond hydroxylation by the $L_5Fe(IV)$═O reagents (Figure 5).[18] Here, for most iron–oxo complexes,[9] the quintet state cuts below the triplet barrier and will participate in product formation. As predicted recently,[9] the extent of participation of the quintet state should decrease as the strength of the C–H bond increases. From the analogous non-heme enzyme TauD, where the C–H bond activation proceeds on the quintet state,[31] the observed KIE value is >30.[31a] This tunneling-like value occurs since the quintet barrier (for cases with weak C–H bonds) is small, on the order of the C–H vibration energy that can propagate the system across the barrier within the amplitude of a single vibration.[9] Therefore, the measurements[32] of KIE values of 30–50 in C–H bond activations of triphenylmethane and ethylbenzene by, for

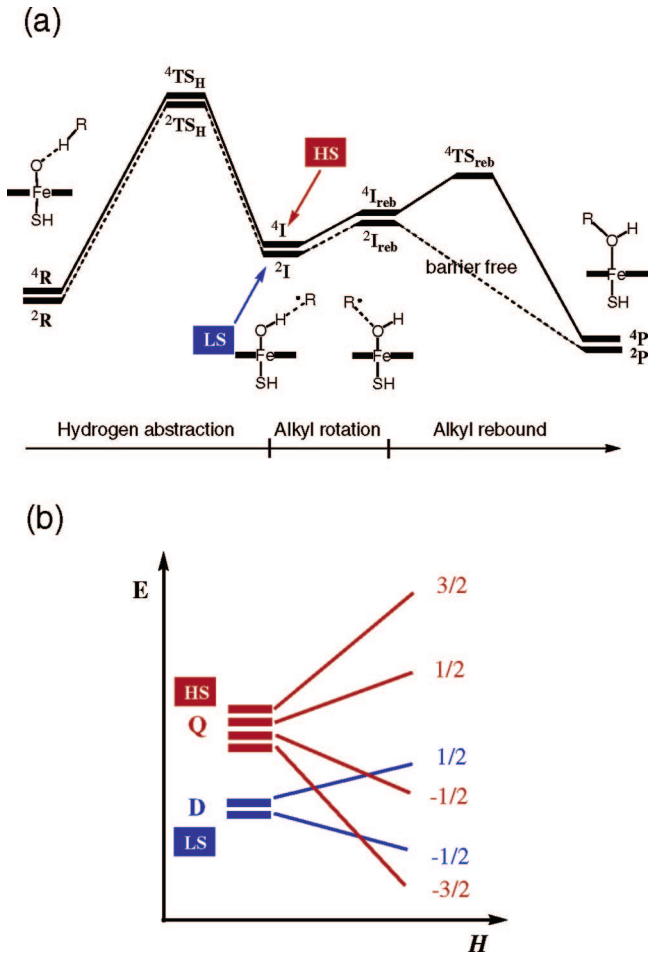

FIGURE 12. (a) Generic TSR in P450 hydroxylation. (b) Effect of magnetic field strength on the spin sublevel energies of the HS and LS intermediates.

example, [N4Py]FeO^{2+} originated in fact in TSR. The TSR prediction[9] that the KIE values should be very large for weaker C–H bonds but normal for cases with stronger C–H bonds is still awaiting a test. Furthermore, using fast radical clocks and measuring KIEs for the rearranged and unrearranged products should reveal major differences in the KIE values for the ***R*** and ***U*** products, differences that are expected to vary also with the strength of the C–H bond.

Magnetic Field Effects in TSR and MSR. As shown in Figures 2,3, and 5, the HS and LS species at the intermediate junction are close in energy. Had the spin inversion in this junction been faster than the rearrangement, all the intermediates would have crossed over to the lowest-energy surface where the reaction is effectively concerted, resulting in complete stereospecificity. The observation of rearranged products, for example, in P450 hydroxylations[2b,26] suggests that spin inversion is slower than rearrangement and rebound. As exemplified in Figure 12, for P450 hydroxylation, a magnetic field will lift the degeneracy of the spin sublevels of the HS-quartet and LS-doublet states, and hence will induce crossings between the spin states, and may thereby affect the spin crossover rates. In such an event, the extent of stereochemical scrambling will vary with the strength of the applied field. Magnetic field effects were demonstrated recently for an oxidation reaction of horseradish peroxidase.[33]

Electric Field and Double-Field Effects in TSR and MSR. External electric fields affect the relative energies of spin states.[34a] For example, when Cpd I reacts with propene, the electric field strength, its direction, and its orientation have selective stabilization effects on the HS and LS transition states of both hydroxylation and epoxidation reactions, as well as on the regiochemical preference for epoxidation versus hydroxylation.[34a] The application of electric fields will also change the relative stability of HS and LS intermediates.[34b] Therefore, double-field experiments, combining electric and magnetic fields, can be utilized to modulate the stereoselectivity and regioselectivity. Electric-field effects, demonstrated in principle for P450,[34a] will be truly spectacular[34b] in highly charged reagents, such as [N4Py]FeO^{2+}, [TMC(L)]$FeO^{1,2+}$, etc.,[2a,18,35] and the functionalized polyoxometalates, e.g., PW_{11}-MnO^{4-}.[17]

Concluding Remarks

This Account focuses on the TSR/MSR concept, its occurrence in the reactions of high-valent metal–oxo reagents, and its manifestations and potential probes. The concept applies well beyond. Our ongoing studies reveal TSR/MSR situations in aziridination and amidation by heme and non-heme iron–nitrido complexes[34b] and in oxidation by vanadium-substituted polyoxometalates. TSR/MSR is also prevalent in a variety of gas-phase and organometallic processes.[22,36]

Concepts are generators of our worlds and the creative means whereby these worlds may change and evolve. The TSR/MSR concept can fashion a mechanistic territory in the surging field of chemical and enzymatic reactivity.

S.S. is supported by the Israel Science Foundation. S.S. thanks his many co-workers in TSR and especially H. Schwarz and D. Schröder with whom this odyssey started. The Account is dedicated to Sigrid Peyerimhoff on her 70th birthday.

References

(1) (a) Ghosh, A. High-Valent Iron Intermediates in Biology. *J. Inorg. Biochem.* **2006**, *100*, 419–880. (b) van Eldik, R. Inorganic and Bioinorganic Mechanisms. *Chem. Rev.* **2005**, *105*, 1917–2722.
(2) (a) Shan, X.; Que, L., Jr. High-Valent Nonheme Iron-Oxo Species in Biomimetic Oxidations. *J. Inorg. Biochem.* **2006**, *100*, 421–433. (b) Groves, J. T. High-Valent Iron in Chemical and Biological Oxidations. *J. Inorg. Biochem.* **2006**, *100*, 434–447.
(3) Derat, E.; Shaik, S. An Efficient Proton-Coupled Electron Transfer Process during Oxidation of Ferulic Acid by Horseradish Peroxidase: Coming Full Cycle. *J. Am. Chem. Soc.* **2006**, *128*, 13940–13949.
(4) Shaik, S.; Kumar, D.; de Visser, S. P.; Altun, A.; Thiel, W. Theoretical Perspective on Structure and Mechanisms of Cytochrome P450 Enzymes. *Chem. Rev.* **2005**, *105*, 2279–2328.
(5) (a) Siegbahn, P. E. M.; Borowski, T. Modeling Enzymatic Reactions Involving Transition Metals. *Acc. Chem. Res.* **2006**, *39*, 729–738. (b) Ryde, U. Combined Quantum and Molecular Mechanics Calculations on Metalloproteins. *Curr. Opin. Chem. Biol.* **2003**, *7*, 136–142.
(6) (a) Shaik, S.; Danovich, D.; Schröder, D.; Schwarz, H. Two-State Reactivity in Organometallic Gas-Phase Ion Chemistry. *Helv. Chim. Acta* **1995**, *78*, 1393–1407. (b) de Visser, S. P.; Ogliaro, F.; Harris,

N.; Shaik, S. Multi-State Epoxidation of Ethene by Cytochrome P450: A Quantum Chemical Study. *J. Am. Chem. Soc.* **2001**, *123*, 3037–3047. (c) Schröder, D.; Shaik, S.; Schwarz, H. Two-State Reactivity as a New Concept in Organometallic Chemistry. *Acc. Chem. Res.* **2000**, *33*, 139–145.

(7) Shaik, S.; Cohen, S.; de Visser, S. P.; Sharma, P. K.; Kumar, D.; Kozuch, S.; Ogliaro, F.; Danovich, D. The "Rebound Controversy": An Overview and Theoretical Modeling of the Rebound Step in C-H Hydroxylation by Cytochrome P450. *Eur. J. Inorg. Chem.* **2004**, *207*, 207–226.

(8) Shaik, S.; Filatov, M.; Schröder, D.; Schwarz, H. Electronic Structure Makes a Difference: Cytochrome P-450 Mediated Hydroxylation of Hydrocarbons as a Two-State Reactivity Paradigm. *Chem.—Eur. J.* **1998**, *4*, 193–199.

(9) Hirao, H.; Kumar, D.; Que, L., Jr.; Shaik, S. Two-State Reactivity in Alkane Hydroxylation by Nonheme Iron-Oxo Complexes. *J. Am. Chem. Soc.* **2006**, *128*, 8590–8606.

(10) Filatov, M.; Shaik, S. Theoretical Investigation of Two-State Reactivity Pathways of H-H Activation by FeO^+: Addition-Elimination, "Rebound" and Oxene-Insertion Mechanisms. *J. Phys. Chem. A* **1998**, *102*, 3835–3846.

(11) (a) Clemmer, D. E.; Chen, Y.-M.; Kahn, F. A.; Armentrout, P. B. State-Specific Reactions of Fe^+ (a^6D,a^4F) with D_2O and Reactions of FeO^+ with D_2. *J. Phys. Chem.* **1994**, *98*, 6522–6529. (b) Fiedler, A.; Schröder, D.; Shaik, S.; Schwarz, H. Electronic Structures and Gas-Phase Reactivities of Cationic Late-Transition-Metal Oxides. *J. Am. Chem. Soc.* **1994**, *116*, 10734–10741.

(12) (a) Yoshizawa, K. Nonradical Mechanism for Methane Hydroxylation by Iron-Oxo Complexes. *Acc. Chem. Res.* **2006**, *39*, 375–382. (b) Shiota, Y.; Yoshizawa, K. Methane-to-Methanol Conversion by First-Row Transition-Metal Oxide Ions: ScO^+, TiO^+, VO^+, CrO^+, MnO^+, FeO^+, CoO^+, NiO^+, and CuO^+. *J. Am. Chem. Soc.* **2000**, *122*, 12317–12326.

(13) Kumar, D.; de Visser, S. P.; Sharma, P. K.; Cohen, S.; Shaik, S. Radical Clock Substrates, Their C-H Hydroxylation Mechanism by Cytochrome P450 and Other Reactivity Patterns: What Does Theory Reveal about Clocks' Behavior. *J. Am. Chem. Soc.* **2004**, *126*, 1907–1920.

(14) Hirao, H.; Shaik, S. Unpublished data .

(15) Poulos, T. L. The Role of the Proximal Ligand in Heme Enzymes. *J. Biol. Inorg. Chem.* **1996**, *1*, 356–359.

(16) Kumar, D.; de Visser, S. P.; Shaik, S. Multi-State Reactivity in the Epoxidation of Styrene by Compound I of Cytochrome P450: Mechanisms of Products and Side Products Formation. *Chem.—Eur. J.* **2005**, *11*, 2825–2835.

(17) Khenkin, A. M.; Kumar, D.; Shaik, S.; Neumann, R. Characterization of Mn(V)-Oxo Polyoxometalate Intermediates and Their Properties in Oxygen Transfer Reactions. *J. Am. Chem. Soc.* **2006**, *128*, 15451–15460.

(18) Bukowski, M. R.; Koehntop, K. D.; Stubna, A.; Bominaar, E. L.; Halfen, J. A.; Münck, E.; Nam, W.; Que, L., Jr. A Thiolate-Ligated Nonheme Oxoiron(IV) Complex Relevant to Cytochrome P450. *Science* **2005**, *310*, 1000–1002.

(19) (a) Carter, E. A.; Goddard, W. A., III. Relationships between Bond Energies in Coordinatively Unsaturated and Coordinatively Saturated Transition-Metal Complexes: A Quantitative Guide for Single, Double, and Triple Bonds. *J. Phys. Chem.* **1988**, *92*, 5679–5683. (b) Carter, E. A.; Goddard, W. A., III. Early- versus Late-Transition-Metal-Oxo Bonds: The Electronic Structure of VO^+ and RuO^+. *J. Phys. Chem.* **1988**, *92*, 2109–2115.

(20) Ogliaro, F.; de Visser, S. P.; Groves, J. T.; Shaik, S. Chameleon States: The High-Valent Metal-Oxo Species of Cytochrome P450 and its Ruthenium Analog. *Angew. Chem., Int. Ed.* **2001**, *40*, 2874–2878.

(21) Hirao, H.; Shaik, S.; Koslowski, P. M. Theoretical Analysis of Structural and Electronic Properties of Metalloporphyrin π-Cation Radicals. *J. Phys. Chem. A* **2006**, *110*, 6091–6099.

(22) Poli, R.; Harvey, J. N. Spin Forbidden Chemical Reactions of Transition Metal Compounds. New Ideas and New Computational Challenges. *Chem. Soc. Rev.* **2003**, *32*, 1–8.

(23) Danovich, D.; Shaik, S. Spin-Orbit Coupling in the Oxidative Activation of H-H by FeO^+. Selection Rules and Reactivity Effects. *J. Am. Chem. Soc.* **1997**, *119*, 1773–1786.

(24) Schröder, D.; Schwarz, H.; Clemmer, D. E.; Chen, Y.; Armentrout, P. B.; Baranov, V. I.; Bohme, D. K. Activation of Hydrogen and Methane by Thermalized FeO^+ in the Gas Phase as Studied by Multiple Mass Spectrometric Techniques. *Int. J. Mass Spectrom. Ion Processes* **1997**, *161*, 175–192.

(25) Newcomb, M.; Toy, P. H. Hypersensitive Radical Probes and the Mechanisms of Cytochrome P450-Catalyzed Hydroxylation Reactions. *Acc. Chem. Res.* **2000**, *33*, 449–455.

(26) For example: (a) Ortiz de Montellano, P. R.; De Voss, J. Oxidizing Species in the Mechanism of Cytochrome P450. *Nat. Prod. Rep.* **2002**, *19*, 477–493. (b) He, X.; Ortiz de Montellano, P. R. Radical Rebound Mechanism in Cytochrome P450-Catalyzed Hydroxylation of the Multifaceted Radical Clocks α- and β-Thujone. *J. Biol. Chem.* **2004**, *279*, 39479–39484.

(27) (a) Bathelt, C. M.; Ridder, L.; Mulholland, A. J.; Harvey, J. N. Mechanism and Structure-Reactivity Relationships for Aromatic Hydroxylation by Cytochrome P450. *Org. Biomol. Chem.* **2004**, *2*, 2998–3005. (b) de Visser, S. P.; Shaik, S. Proton-Shuttle Mechanism Mediated by the Porphyrin in Benzene Hydroxylation by Cytochrome P450 Enzymes. *J. Am. Chem. Soc.* **2003**, *125*, 7413–7425.

(28) Li, C.; Wu, W.; Kumar, D.; Shaik, S. Kinetic Isotope Effect is a Sensitive Probe of Spin State Reactivity in C-H Hydroxylation of *N,N*-dimethylaniline by Cytochrome P450. *J. Am. Chem. Soc.* **2006**, *128*, 394–395.

(29) Harris, N.; Shaik, S.; Schröder, D.; Schwarz, H. Single- and Two-State Reactivity in the Gas Phase C-H Bond Activation of Norbornane by Bare FeO^+. *Helv. Chim. Acta* **1999**, *82*, 1784–1797.

(30) Manchester, J. I.; Dinnocenzo, J. P.; Higgins, L. A.; Jones, J. P. A New Mechanistic Probe for Cytochrome P450: An Application of Isotope Effect Profiles. *J. Am. Chem. Soc.* **1997**, *119*, 5069–5070.

(31) (a) Price, J. C.; Barr, E. W.; Glass, T. E.; Krebs, C.; Bollinger, J. M., Jr. Evidence for Hydrogen Abstraction from C1 of Taurine by High-Spin Fe(IV) Intermediate Detected during Oxygen Activation by Taurine:α-Ketoglutarate Dioxygenase (TauD). *J. Am. Chem. Soc.* **2003**, *125*, 13008–13009. (b) de Visser, S. P. Propene Activation by the Iron-Oxo Active Species of Taurine/α-Ketoglutarate Dioxygenase (TauD) Enzyme. How Does the Catalysis Compare to Heme-Enzymes? *J. Am. Chem. Soc.* **2006**, *128*, 9813–9824.

(32) Kaizer, J.; Klinker, E. J.; Oh, N. Y.; Rhode, J.-U.; Song, W. J.; Stubna, A.; Kim, J.; Münck, E.; Nam, W.; Que, L., Jr. Noneheme $Fe^{IV}O$ Complexes That Can Oxidize the C-H Bonds of Cyclohexane at Room Temperature. *J. Am. Chem. Soc.* **2004**, *126*, 472–473.

(33) Afanasyeva, M. S.; Taraban, M. B.; Purtov, P. A.; Leshina, T. V.; Grissom, C. B. Magnetic Spin Effects in Enzymatic Reactions: Radical Oxidation of NADPH by Horseradish Peroxidase. *J. Am. Chem. Soc.* **2006**, *128*, 8651–8658.

(34) (a) Shaik, S.; de Visser, S. P.; Kumar, D. An External Electric Field Will Control the Selectivity of an Enzymatic-Like Bond Activations. *J. Am. Chem. Soc.* **2004**, *126*, 11746–11749. (b) Hirao, H.; Shaik, S. Unpublished data .

(35) Bukowski, M. R.; Comba, P.; Lienke, A.; Limberg, C.; Lopez De Lardon, C.; Merz, M.; Que, L., Jr. Catalytic Epoxidation and 1,2-Dihydroxylation of Olefins with Bispidine Iron(II)/H_2O_2 Systems. *Angew. Chem., Int. Ed.* **2006**, *45*, 3446–3449.

(36) A tiny sample: (a) Harvey, J. N.; Poli, R.; Smith, K. M. Understanding of Transition Metal Complexes Involving Multiple Spin States. *Coord. Chem. Rev.* **2003**, *238–239*, 347–361. (b) Schwarz, H. On the Spin-Forbiddeness of Gas Phase Ion-Molecule Reactions: A Fruitful Intersection of Experimental and Computational Studies. *Int. J. Mass Spectrom.* **2004**, *237*, 75–105. (c) Hess, J. S.; Leelasubcharoen, S. L.; Rheingold, A. L.; Doren, D. J.; Theopold, K. H. Spin Surface Crossing in Chromium-Mediated Olefin Epoxidation with O_2. *J. Am. Chem. Soc.* **2002**, *124*, 2454–2455. (d) Döhring, A.; Jensen, V. R.; Jolly, P. W.; Thiel, W.; Weber, J. C. Donor-Ligand-Substituted Cyclopentadienylchromium(III) Complexes: A New Class of Alkene Polymerization Catalyst. 2. Phosphinoalkyl-Substituted Systems. *Organometallics* **2001**, *20*, 2234–2245. (e) Strassner, T.; Houk, K. N. Predictions of Geometries and Multiplicities of the Manganese-Oxo Intermediates in the Jacobsen Epoxidation. *Org. Lett.* **1999**, *1*, 419–422. (f) Linde, C.; Koliaï, N.; Norrby, P.-O.; Åkermark, B. Experimental Evidence for Multiple Oxidation Pathways in the (Salen)Mn-Catalyzed Epoxidation of Alkene. *Chem.—Eur. J.* **2002**, *8*, 2568–2573. (g) Jin, N.; Groves, J. T. Unusual Kinetic Stability of a Ground-State Singlet Oxomanganese(V) Porphyrin. Evidence for a Spin State Crossing Effect. *J. Am. Chem. Soc.* **1999**, *121*, 2923–2924.

AR600042C